Synthesis and Biologic Evaluation of ^{64}Cu-Labeled Rhenium-Cyclized α-MSH Peptide Analog Using a Cross-Bridged Cyclam Chelator

Lihui Wei[1], Clayton Butcher[2], Yubin Miao[2], Fabio Gallazzi[2], Thomas P. Quinn[2], Michael J. Welch[1], and Jason S. Lewis[1]

[1]Division of Radiological Sciences, Mallinckrodt Institute of Radiology and the Alvin J. Siteman Cancer Center, Washington University School of Medicine, St. Louis, Missouri; and [2]Department of Biochemistry, University of Missouri-Columbia, Columbia, Missouri

Early detection of cutaneous melanoma is essential, as prognosis with metastatic melanoma is poor. Previous studies showed that ^{64}Cu-DOTA-ReCCMSH(Arg^{11}) (DOTA is 1,4,7,10-tetraazacyclododecane-*N,N′,N″,N‴*-tetraacetic acid), a cyclic analog of α-melanocyte-stimulating hormone (α-MSH), has the potential for the detection of malignant melanoma using PET. However, ^{64}Cu-DOTA-ReCCMSH(Arg^{11}) demonstrated high background in nontarget tissues due to the in vivo instability of the Cu-DOTA moiety. CBTE2A (CBTE2A is 4,11-bis(carboxymethyl)-1,4,8,11-tetraazabicyclo[6.6.2]hexadecane) has been shown to be a more stable copper chelate with improved in vivo stability, resulting in an improvement in clearance from nontarget tissues. The goal of this study was to conjugate CBTE2A to the α-MSH targeting ReCCMSH(Arg^{11}) peptide for labeling to ^{64}Cu and to investigate whether the increased metal-chelate stability with CBTE2A would improve imaging quality. **Methods:** The recyclized peptide CBTE2A-ReCCMSH(Arg^{11}) was synthesized using a solid-phase peptide synthesizer followed by rhenium cyclization. In vivo characteristics of ^{64}Cu-CBTE2A-ReCCMSH(Arg^{11}) were examined with small-animal PET and acute biodistribution studies in B16/F1 tumor-bearing mice. **Results:** Biodistribution studies showed high and rapid receptor-mediated tumor uptake with values similar to those reported for ^{64}Cu- and ^{86}Y-labeled DOTA-ReCCMSH(Arg^{11}). Nontarget organ concentration for ^{64}Cu-CBTE2A-ReCCMSH(Arg^{11}) was considerably lower than that of the ^{64}Cu-DOTA analog, resulting in significantly higher tumor-to-nontarget tissue ratios. Compared with ^{86}Y-DOTA-ReCCMSH(Arg^{11}), ^{64}Cu-CBTE2A-ReCCMSH(Arg^{11}) demonstrated increased tumor retention and kidney clearance. Small-animal PET images showed that the tumor could be clearly visualized at all time points (0.5–24 h). **Conclusion:** Our data suggest the superior stability of the ^{64}Cu-CBTE2A moiety compared with ^{64}Cu-DOTA, making ^{64}Cu-CBTE2A-ReCCMSH(Arg^{11}) an ideal candidate for the PET of malignant melanoma.

Key Words: melanoma; α-melanocyte-stimulating hormone; small-animal PET; ^{64}Cu

J Nucl Med 2007; 48:64–72

Received Jul. 21, 2006; revision accepted Oct. 12, 2006.

For correspondence or reprints contact: Jason S. Lewis, PhD, Mallinckrodt Institute of Radiology, Washington University School of Medicine, 510 S. Kingshighway Blvd., Campus Box 8225, St. Louis, MO 63110.

E-mail: j.s.lewis@wustl.edu

Epidemiologic surveys have demonstrated that the incidence and mortality rates of cutaneous melanoma are still increasing in the United States, as they are in most countries (*1*). Among young adults, melanoma is currently the most common malignancy (*2*), which increases with age (*3*). In 2004 within the United States there were an estimated 55,000 cases of melanoma, of which nearly 8,000 would prove to be fatal (*4*). Unless tumors are detected early and adequate surgery can be performed, the prognosis of this disease is poor (*4*).

^{18}F-FDG nonspecifically localizes in melanoma by being transported into cells that are metabolically active before becoming trapped intercellularly. As cancerous cells typically have a higher metabolic rate than normal cells, they exhibit increased accumulation of ^{18}F-FDG (*5*). However, ^{18}F-FDG PET is limited in detecting melanoma tumors with small foci (*6*), and some melanoma cells are undetectable with ^{18}F-FDG because they use substrates other than glucose as an energy source (*7*).

We previously reported the labeling of DOTA-ReCCMSH(Arg^{11}) (DOTA is 1,4,7,10-tetraazacyclododecane-*N,N′,N″,N‴*-tetraacetic acid) with β^+-emitting radiometals to determine whether it is a viable agent for the detection of malignant melanoma via PET (*8*). We chose the divalent metal ion ^{64}Cu (half-life [$t_{1/2}$] = 12.7 h, 17.4% β^+, 41% electron capture, 40% β^-) (*9*) and the trivalent metal ion ^{86}Y ($t_{1/2}$ = 14.7 h, 33% β^+), both of which can be prepared on a biomedical cyclotron using the ^{64}Ni(p,n)^{64}Cu and ^{86}Sr(p,n)^{86}Y reactions, respectively (*10,11*). Our results showed that both ^{64}Cu-DOTA-ReCCMSH(Arg^{11}) and ^{86}Y-DOTA-ReCCMSH(Arg^{11}) have the potential for the detection of malignant melanoma by exploiting the sensitivity and high resolution of PET (*8*). ^{64}Cu-DOTA-ReCCMSH(Arg^{11}) clearly delineated the tumor within 30 min after injection in the small-animal PET study. However, the acute biodistribution study and small-animal PET showed that ^{64}Cu-DOTA-ReCCMSH(Arg^{11}) demonstrated a higher accumulation of activity in nontarget tissues and clearance organs. This is due to the release of uncoordinated

^{64}Cu from nonextracted complex by decomposition in the blood or transchelation in the liver, causing elevated uptake in these tissues (*12,13*). New cross-bridged cyclam chelates have recently been developed for ^{64}Cu (*14*) that have shown significant metal-chelate stability and, as a consequence, a lowering in nontarget tissue accumulation (*12,15*). It was shown that ^{64}Cu-CBTE2A-Tyr^3-octreotate (where CBTE2A = 4,11-bis(carboxymethyl)-1,4,8,11-tetraazabicyclo[6.6.2]hexadecane) has improved blood, liver, and kidney clearance compared with the analogous ^{64}Cu-TETA (^{64}Cu-1,4,8,11-tetraazacyclotetradecane-*N,N′,N″,N‴*-tetraacetic acid) agent (*15*). Therefore, CBTE2A is an attractive bifunctional chelator for attaching ^{64}Cu to peptides for tumor imaging and radiotherapy.

Herein we report the in vivo biodistribution and small-animal PET studies and an in vitro binding affinity study of ^{64}Cu-CBTE2A-ReCCMSH(Arg^{11}) in the B16/F1 tumor model. We also compare the biologic properties of ^{64}Cu-CBTE2A-ReCCMSH(Arg^{11}) with ^{64}Cu- and ^{86}Y-DOTA-ReCCMSH(Arg^{11}) (Fig. 1).

MATERIALS AND METHODS

Unless otherwise stated, all chemicals were purchased from Sigma-Aldrich Chemical Co. Water was distilled and then deionized (18 MΩ/cm^2) by passing through a Milli-Q water filtration system (Millipore Corp.). CBTE2A was obtained from Dr. Gary R. Weisman and Dr. Edward H. Wong (University of New Hampshire, Durham, NH). ^{64}Cu and ^{86}Y were produced on a CS-15 biomedical cyclotron at Washington University School of Medicine (*10,11*). Radio-TLC (TLC is thin-layer chromatography) detection was accomplished using a BIOSCAN AR2000 imaging scanner.

Bis-Trifluoroacetic Acid Salt of CBTE2A

The bis-trifluoroacetic acid salt of CBTE2A was synthesized according to the published method (*15*).

Synthesis of CBTE2A-ReCCMSH (Arg^{11})

CBTE2A-CCMSH(Arg^{11}) was synthesized using standard Fmoc/HBTU (HBTU = *O*-benzotriazole-*N,N,N′,N′*-tetramethyl-uranium-hexafluoro-phosphate) chemistry on an amide resin with an Advanced ChemTech Omega 396 multiple peptide synthesizer (Advanced ChemTech). The CBTE2A chelator was obtained from the *tert*-Bu−protected precursor by treatment with 50% trifluoroacetic acid (TFA) in dichloromethane and then conjugated to the N terminus of the CCMSH(Arg^{11}) peptide while on the resin (Rink Amide NovaGel; Novabiochem) according to previously published procedures (*15*). Peptide cleavage and deprotection were achieved by treating the peptidyl-resin for 3 h with a mixture of TFA, thioanisole, phenol, water, ethanedithiol, and triisopropylsilane (87.5:2.5:2.5:2.5:2.5:2.5). CBTE2A-CCMSH(Arg^{11}) was cyclized via site-specific rhenium coordination. Twenty milligrams of linear CBTE2A-CCMSH(Arg^{11}) were dissolved in 800 μL of *N,N*-dimethylformamide (DMF). An equal molar quantity of trichlorooxobis-(triphenylphosphine)-rhenium(V) (Aldrich Chemical) was dissolved in 1 mL of DMF and added to the CBTE2A-CCMSH(Arg^{11}) solution. DMF was added to the reaction solution to yield a final peptide concentration of 4 mg/mL, and the solution was shaken at 25°C for 3 h. CBTE2A-ReCCMSH (Arg^{11}) was purified on Beckman-Coulter System Gold high-performance liquid chromatography (HPLC) using a Prep NovaPak, HR-C_{18} reverse-phase column (Waters) with a 40-min gradient of 20%–40% 0.1% TFA/acetonitrile versus 0.1% TFA/H_2O with a 10 mL/min

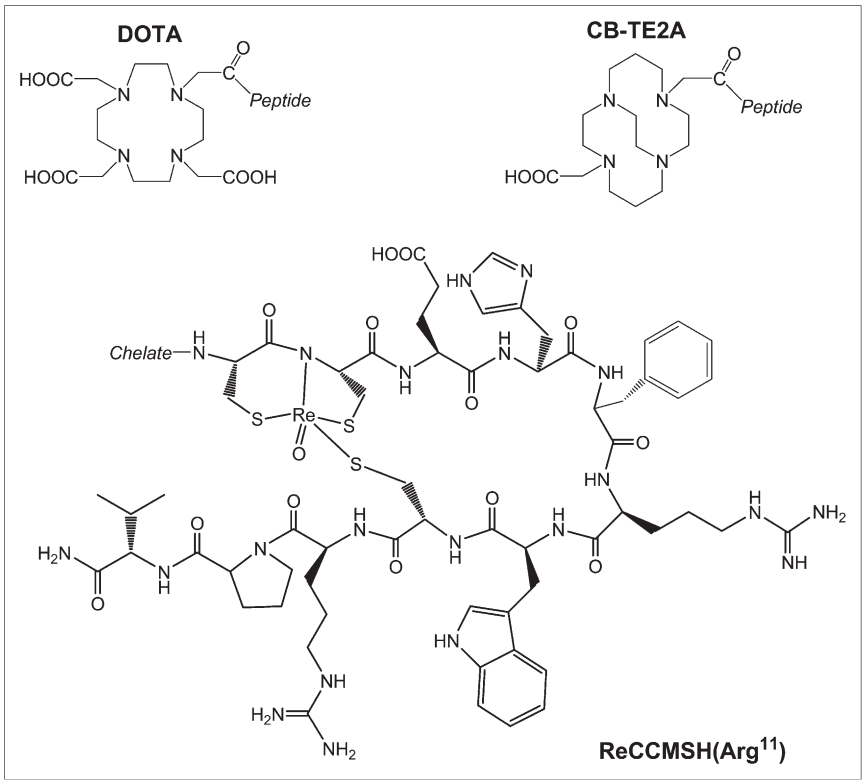

FIGURE 1. Structures of CBTE2A-ReCCMSH(Arg^{11}) and DOTA-ReCCMSH(Arg^{11}).

flow rate. The identity of the purified sample was verified using a liquid chromatography–mass spectrometer, and the sample was lyophilized.

Radiolabeling of CBTE2A-ReCCMSH(Arg^{11})

^{64}Cu (18.5–148 MBq [0.5–4 mCi]) in 0.1 mol/L ammonium acetate (pH 8.0) was added to 2 μg of CBTE2A-ReCCMSH(Arg^{11}) in 0.1 mol/L ammonium acetate (pH 8.0). The reaction mixture was incubated at 95°C for 1 h. The reaction was monitored by radio-TLC using Whatman $MKC_{18}F$ TLC plates developed with 30:70 10% NH_4OAc/ methanol (^{64}Cu-CBTE2A-ReCCMSH(Arg^{11}) R_f = 0.4). The ^{64}Cu-labeled peptide was further purified (if required) by reverse-phase HPLC (RP-HPLC) using a Microsorb C_{18}, 4.6 × 250 mm column (Varian Inc.) eluted with a linear gradient of 15%–21% acetonitrile in 0.1% TFA over 55 min at a flow rate of 1.0 mL/min. ^{64}Cu-CBTE2A-ReCCMSH(Arg^{11}) (retention time [t_R] = 42 min) was collected in 1–2 mL of HPLC solvent. The solvent was then removed and reconstituted in saline.

In Vitro Competitive Binding Assay

The 50% inhibitory concentration (IC_{50}) for Cu-CBTE2A-ReCCMSH(Arg^{11}) was determined by using methods described previously (*16,17*). B16/F1 cells (5 ×10^5 per well) were seeded into sterile 24-well plates in RPMI 1640 medium containing $NaHCO_3$ (2 g/L), supplemented with 10% heat-inactivated fetal calf serum, 2 mmol/L L-glutamine, and 48 mg gentamicin and incubated at 37°C overnight. After being washed once with binding medium (minimum essential medium with 25 mmol/L *N*-(2-hydroxyethyl)piperazine-*N*′-(2-ethanesulfonic acid), pH 7.4, 0.2% bovine serum albumin [BSA], 0.3 mmol/L 1,10-phenathroline), the cells were incubated at room temperature (25°C) for 2 h with approximately 50,000 cpm of ^{125}I-Tyr^2-NDP (NDP is [Nle^4,D-Phe^7]) (Amersham Pharmacia Biotech) in the presence of increasing concentrations of Cu-CBTE2A-ReCCMSH(Arg^{11}) in 0.3 mL of binding medium. Cells were rinsed with 0.5 mL of ice-cold, pH 7.4, 0.2% BSA/0.01 mol/L phosphate-buffered saline twice and lysed in 0.5 mL of 1N NaOH for 5 min. The activity in cells was measured in a NaI well counter. The competitive binding curve was obtained by plotting the percentage of ^{125}I-Tyr^2-NDP bound to cells versus concentrations of displacing peptide. The IC_{50} value for the peptide was calculated by using the Grafit software (Erithacus Software Ltd.).

Biodistribution Studies

All animal experiments were conducted in compliance with the Guidelines for the Care and Use of Research Animals established by Washington University's Animal Studies Committee. Biodistribution studies were performed on 18- to 23-g female C57 BL/6 mice (Charles River Laboratories) that had been implanted with 1 × 10^6 cultured B16/F1 murine melanoma cells subcutaneously into the nape of the neck. Tumors were allowed to grow for 10 d (~0.3–0.7 cm^3), at which time the animals received 0.20 MBq (~5 μCi) of ^{64}Cu-CBTE2A-ReCCMSH(Arg^{11}) in 100 μL of saline via lateral tail vein injection. Two groups were examined at 4 time points (n = 5 per group at 30 min and at 2, 4, and 24 h), with each group receiving different specific activities (SAs). The first cohort received 16 ng (22.2 GBq/μmol) of peptide so that a direct comparison could be made with ^{64}Cu-DOTA-ReCCMSH(Arg^{11}) (*8*). A second cohort received 2 ng (185 GBq/μmol) of peptide to observe the optimal biodistribution at the highest achievable SA. To examine in vivo uptake specificity, a third group of mice (2-h time point only) was preinjected with unlabeled peptide (20 μg [10.3 nmol] of CBTE2A-ReCCMSH(Arg^{11})) to act as a receptor blockade immediately before administering ^{64}Cu-CBTE2A-ReCCMSH(Arg^{11}) (16 ng). This represents a 1,250-fold increase over the mass of peptide injected with ^{64}Cu-CBTE2A-ReCCMSH(Arg^{11}). In an attempt to reduce kidney uptake and retention, a fourth group of mice (2-h time point only) was preinjected with 15 mg of D-lysine immediately before administering ^{64}Cu-CBTE2A-ReCCMSH(Arg^{11}) (16 ng). In all studies after euthanasia, tissues and organs of interest were removed and weighed, and the radioactivity was measured in a γ-counter. The percentage injected dose per gram (%ID/g) was then calculated on comparison with known standards.

Small-Animal PET Studies

Whole-body small-animal PET was performed on a microPET Focus scanner (Siemens Medical Solutions) (*18*). Imaging studies were also performed on C57 BL/6 mice bearing day-10 B16/F1 murine melanoma tumors. The mice were injected via the tail vein with ^{64}Cu-CBTE2A-ReCCMSH(Arg^{11}) (5.5 MBq, 500 ng). These mice were imaged side by side with mice that had been treated with 20 μg of unlabeled peptide (as a blockade) immediately before injection of ^{64}Cu-CBTE2A-ReCCMSH(Arg^{11}). At 0.5, 2, 4, and 24 h after injection, the mice were anesthetized with 1%–2% isoflurane, positioned supine, immobilized, and imaged. Tumor, kidney, and liver standardized uptake values (SUVs) were generated by measuring regions of interest that encompassed the entire organ from the PET images.

Statistical Methods

All data are presented as mean ± SD. For statistical classification, a Student t test was performed using GraphPad PRISM. Differences at the 95% confidence level ($P < 0.05$) were considered significant.

RESULTS

Synthesis of CBTE2A-ReCCMSH(Arg^{11})

Linear CCMSH(Arg^{11}) peptide was prepared using standard solid-phase peptide synthesis techniques. The CBTE2A chelator was appended to the N terminus of the CCMSH(Arg^{11}) peptide during the final step of peptide synthesis. CBTE2A-CCMSH(Arg^{11}) was cleaved from the resin and deprotected. Crude CBTE2A-CCMSH(Arg^{11}) was cyclized through site coordination of rhenium via a transchelation reaction. It was necessary to synthesize CBTE2A-ReCCMSH(Arg^{11}) in DMF at room temperature as opposed to 60% MeOH at 70°C, which was used for DOTA-ReCCMSH(Arg^{11}). Differences in charge, hydrophobicity, and steric interactions between the chelator and the peptide appeared to result in the necessity of different solution conditions for the CBTE2A-CCMSH(Arg^{11}) rhenium cyclization reaction. CBTE2A-ReCCMSH(Arg^{11}) was purified by reverse-phase HPLC, lyophilized, and stored at −20°C. The identify of the uncyclized and the purified CBTE2A-ReCCMSH(Arg^{11}) compound was verified by LC-mass spectroscopy (CBTE2A-CCMSH(Arg^{11}) m/z calculated for $C_{78}H_{120}N_{25}O_{16}S_3$ = 1,758.85, found m/2 = 880.86; CBTE2A-ReCCMSH m/z calculated for $C_{78}H_{116}N_{25}O_{17}ReS_3$ = 1,957.77, found m/2 = 979.86).

Radiolabeling of CBTE2A-ReCCMSH(Arg^{11}) with ^{64}Cu

CBTE2A-ReCCMSH(Arg^{11}) was successfully labeled with ^{64}Cu in ammonium acetate buffer (pH 8.0) at 95°C for 1 h. Different amounts of ^{64}Cu were added to achieve different SAs. These conditions are different from those required for the DOTA analog (0.1 mol/L NaOAc, pH 5.5, at 65°C for 1 h) (*8*). The labeled peptide was separated from unlabeled peptide by RP-HPLC as required. ^{64}Cu-CBTE2A-ReCCMSH (t_R = 42 min) was obtained with a radiochemical purity of >98% and SAs ranging from 22.2 to 185 GBq/μmol. The unlabeled CBTE2A-ReCCMSH was eluted under the same HPLC conditions with a t_R of 36 min and unreacted ^{64}Cu was eluted in the void volume.

In Vitro Competitive Binding Assay

The IC_{50} for nonradioactive Cu-CBTE2A-ReCCMSH(Arg^{11}) was determined by an in vitro competitive binding assay and compared with that of nonradioactive Cu-DOTA-ReCCMSH(Arg^{11}). The IC_{50} for Cu-CBTE2A-ReCCMSH(Arg^{11}) was 5.4 ± 0.59 nmol/L, whereas Cu-DOTA-ReCCMSH(Arg^{11}) yielded an IC_{50} of 6.9 nmol/L. Substitution of the DOTA chelator by the CBTE2A chelator did not appear to affect melanocortin-1 receptor (MC1R) binding of the conjugated peptide.

Animal Biodistribution Studies

The in vivo biodistribution of ^{64}Cu-CBTE2A-ReCCMSH(Arg^{11}) was examined in female C57 BL/6 mice bearing day-10 B16/F1 murine melanoma tumors. Table 1 presents the biodistribution data at 30 min and at 2, 4, and 24 h after injection for ^{64}Cu-CBTE2A-ReCCMSH (185 kBq [5 μCi], 16 ng). An additional group was preinjected with unlabeled peptide to act as a blockade (20 μg of CBTE2A-ReCCMSH(Arg^{11}), 10.3 nmol) and mice were sacrificed at 2 h after injection. The tumor accumulation of ^{64}Cu-CBTE2A-ReCCMSH reached a maximum after 30 min (8.45 ± 1.42 %ID/g) and the tumor retention was high, with 7.09 ± 3.20 and 7.37 ± 1.26 %ID/g remaining at 2 and 4 h, respectively. After 24 h, the tumor concentration only decreased by ~2-fold (24 h, 4.01 ± 0.77 %ID/g; $P < 0.005$). Preinjection with 20 μg of CBTE2A-ReCCMSH(Arg^{11}) significantly reduced tumor uptake of the radiolabeled peptide (0.99 ± 0.15 %ID/g; $P < 0.005$) at 2 h after injection, strongly supporting a receptor-mediated uptake of the radiolabeled peptide. The other organs excised demonstrated no major significant differences between the group that received blockade and the group that did not. The subtle increase in tracer uptake in nontarget organs can be attributed to slightly elevated levels of radioactivity in the blood. The reason for higher levels of activity in the blood could be attributed to lower levels of accumulation in the tumor.

Figure 2 illustrates a comparison of the biodistribution properties between ^{64}Cu-CBTE2A- and ^{64}Cu-DOTA-ReCCMSH(Arg^{11}) (*8*) with a similar mass (16 ng) of radiolabeled peptides at all time points. The biodistribution data showed that the radioactive background in the blood and blood-rich content organs, such as liver, lung, heart, and spleen, for ^{64}Cu-CBTE2A-ReCCMSH(Arg^{11}) was significantly lower than that for ^{64}Cu-DOTA analog. For example, the liver uptake was 3- to 5-fold lower for ^{64}Cu-CBTE2A-ReCCMSH(Arg^{11}) than that for ^{64}Cu-DOTA-ReCCMSH(Arg^{11}) at all time points (e.g., at 2 h, ^{64}Cu-CBTE2A-ReCCMSH(Arg^{11}), 1.57 ± 0.42 %ID/g, vs. ^{64}Cu-DOTA-ReCCMSH(Arg^{11}), 7.25 ± 1.02 %ID/g, $P < 0.001$; at 24 h, ^{64}Cu-CBTE2A-ReCCMSH(Arg^{11}), 1.00 ± 0.09 %ID/g, vs. ^{64}Cu-DOTA-ReCCMSH(Arg^{11}), 4.85 ± 1.52 %ID/g, $P < 0.01$). ^{64}Cu-CBTE2A-ReCCMSH(Arg^{11}) also demonstrated significantly faster blood clearance compared with ^{64}Cu-DOTA-ReCCMSH(Arg^{11}). This resulted in 6- and 7.5-fold lower blood activity at 4 and 24 h, respectively, for ^{64}Cu-CBTE2A-ReCCMSH(Arg^{11}) compared with the DOTA analog (4 h, $P < 0.0005$; 24 h, $P < 0.005$). The muscle uptake was also lower for ^{64}Cu-CBTE2A-ReCCMSH(Arg^{11}) than that for ^{64}Cu-DOTA analog at 2-, 4-, and 24-h time points (i.e., at 4 h, ^{64}Cu-CBTE2A-ReCCMSH(Arg^{11}), 0.07 ± 0.04 %ID/g, vs. ^{64}Cu-DOTA-ReCCMSH(Arg^{11}), 0.32 ± 0.04 %ID/g, 4.5

TABLE 1
Biodistribution of ^{64}Cu-CBTE2A-ReCCMSH(Arg^{11}) (16 ng) (%ID/g ± SD, n = 5) in C57BL/6 Mice Bearing Day-10 B16/F1 Melanoma Tumors at 30 Minutes and at 2, 4, and 24 Hours

Tissue	30 min	2 h	2 h with blockade*	4 h	24 h
Blood	2.95 ± 1.11	0.19 ± 0.04	0.47 ± 0.15	0.11 ± 0.03	0.06 ± 0.03
Lung	3.29 ± 1.16	0.53 ± 0.06	0.91 ± 0.16	0.33 ± 0.07	0.14 ± 0.03
Liver	2.37 ± 0.28	1.57 ± 0.42	1.74 ± 0.52	1.77 ± 0.12	1.00 ± 0.09
Spleen	0.89 ± 0.11	0.34 ± 0.08	0.44 ± 0.12	0.34 ± 0.05	0.20 ± 0.04
Kidney	12.71 ± 1.50	8.57 ± 2.51	11.05 ± 3.26	6.92 ± 1.05	3.62 ± 0.27
Muscle	1.25 ± 0.34	0.16 ± 0.04	0.28 ± 0.11	0.07 ± 0.04	0.05 ± 0.03
Heart	1.32 ± 0.37	0.21 ± 0.01	0.31 ± 0.09	0.12 ± 0.03	0.06 ± 0.03
Skin	4.42 ± 0.89	0.53 ± 0.22	1.36 ± 0.31	0.25 ± 0.03	0.08 ± 0.04
B16/F1 tumor	8.45 ± 1.42	7.09 ± 3.20	0.99 ± 0.15	7.37 ± 1.26	4.01 ± 0.77

*An additional group was pretreated with blockade (20 μg CBTE2A-ReCCMSH(Arg^{11})).

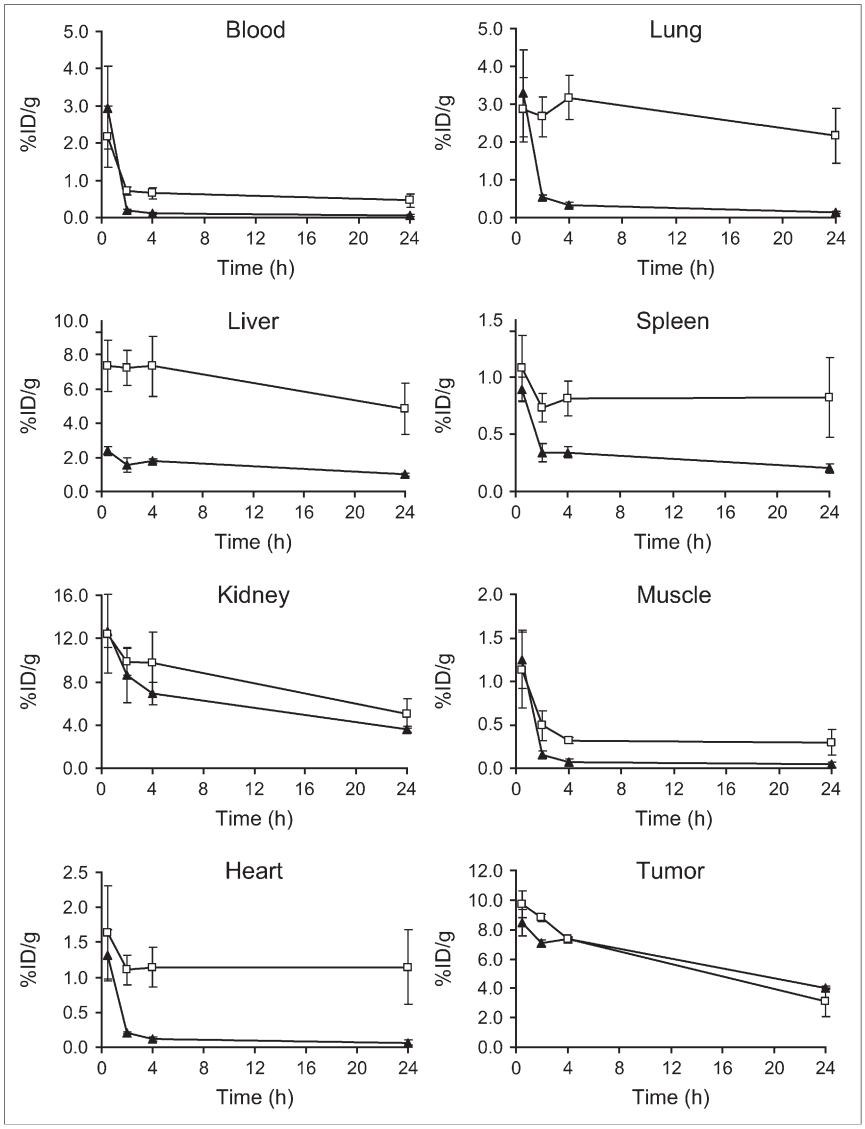

FIGURE 2. Comparison of biodistribution of ^{64}Cu-DOTA-ReCCMSH(Arg^{11}) (185 kBq [5 μCi], 16 ng, $n = 4$; □) (*8*) and ^{64}Cu-CBTE2A-ReCCMSH(Arg^{11}) (185 kBq [5 μCi], 16 ng, $n = 5$; ▲) in B16/F1 tumor-bearing C57 mice at 2 h after injection. Data are presented as %ID/g ± SD. Note differences in *y*-axis scales.

times lower, $P < 0.00001$; at 24 h, ^{64}Cu-CBTE2A-ReCCMSH(Arg^{11}), 0.05 ± 0.03 %ID/g, vs. ^{64}Cu-DOTA-ReCCMSH(Arg^{11}), 0.30 ± 0.15 %ID/g, 6 times lower, $P < 0.05$). The kidney uptake at 30 min was not significantly different between ^{64}Cu-CBTE2A-ReCCMSH(Arg^{11}) and ^{64}Cu-DOTA-ReCCMSH(Arg^{11}) (^{64}Cu-CBTE2A-ReCCMSH(Arg^{11}), 12.71 ± 1.50 %ID/g, vs. ^{64}Cu-DOTA-ReCCMSH(Arg^{11}), 12.43 ± 3.62 %ID/g, P = not significant [NS]). However, the kidney clearance of ^{64}Cu-CBTE2A-ReCCMSH(Arg^{11}) is a little faster than that of the ^{64}Cu-DOTA-ReCCMSH(Arg^{11}), resulting in 1.4 times higher kidney uptake of ^{64}Cu-DOTA-ReCCMSH(Arg^{11}) at 24 h compared with ^{64}Cu-CBTE2A-ReCCMSH(Arg^{11}) ($P < 0.05$). Tumor uptake of the 2 complexes is not statistically different at any time point (e.g., at 4 h, ^{64}Cu-CBTE2A-P, 7.37 ± 1.26 %ID/g, vs. ^{64}Cu-DOTA-P, 7.35 ± 1.47 %ID/g, P = NS).

Another study investigated whether the SA of the radiolabeled peptide would affect the tumor accumulation and the uptake in other organs. By adding different amounts of ^{64}Cu, we were able to isolate ^{64}Cu-CBTE2A-ReCCMSH-(Arg^{11}) with lower SA (22.2 GBq/μmol) and with higher SA (185 GBq/μmol) and to compare their biodistribution properties at 2 h after injection (Fig. 3). We found that increasing SA significantly increased tumor concentration by 3.2-fold (from 7.09 ± 3.20 %ID/g to 22.59 ± 2.99 %ID/g; $P < 0.005$). The uptake of nontarget organs, such as kidney, liver, and blood uptake, was also increased (1.6- to 2-fold), but not as significantly as the increase in tumor uptake (kidney uptake, low SA: 8.57 ± 2.51 %ID/g vs. high SA: 13.71 ± 1.17 %ID/g, $P < 0.05$; liver uptake, low SA: 1.57 ± 0.42 %ID/g vs. high SA: 2.49 ± 0.29 %ID/g, $P < 0.05$; blood uptake, low SA: 0.19 ± 0.04 %ID/g vs. high SA: 0.48 ± 0.22 %ID/g, $P < 0.05$). We also studied the effect of lysine on kidney uptake (Fig. 3). We found that administration of 15 mg of D-lysine dramatically reduced the kidney uptake by 2.4-fold (from 13.71 ± 1.17 %ID/g to 5.85 ± 1.14 %ID/g; $P < 0.0001$). However, surprisingly,

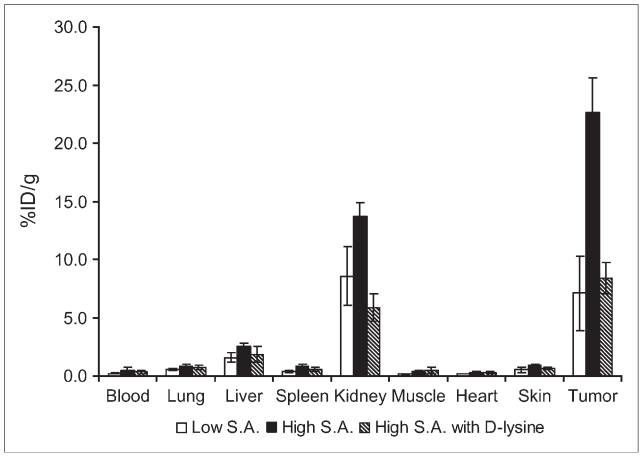

FIGURE 3. Biodistribution comparison of ^{64}Cu-CBTE2A-ReCCMSH(Arg^{11}) with high SA (2 ng) and low SA (16 ng) and effect of preinjection of 15 mg D-lysine (2 h after injection).

the tumor uptake was also decreased by the same extent (from 22.59 ± 2.99 %ID/g to 8.39 ± 1.37 %ID/g; $P < 0.005$). No other organs demonstrated significant differences between the group that received lysine and the group that did not.

Figure 4 shows the comparison of the biodistribution data obtained from ^{64}Cu-CBTE2A-, ^{64}Cu-DOTA-, and ^{86}Y-DOTA-ReCCMSH(Arg^{11}) (*8*) with selected tumor-to-nontarget organ ratios (2 h after injection). As discussed earlier, the uptake of nontarget tissues is lower for ^{64}Cu-CBTE2A-ReCCMSH(Arg^{11}) compared with that of ^{64}Cu-DOTA-ReCCMSH(Arg^{11}), whereas the tumor uptake is close to each other, so it is apparent that there is a significant increase in the tumor-to-nontarget organ ratios for ^{64}Cu-CBTE2A-ReCCMSH(Arg^{11}) when compared with ^{64}Cu-DOTA-ReCCMSH(Arg^{11}). ^{64}Cu-CBTE2A-ReCCMSH(Arg^{11}) with higher SA demonstrated higher tumor-to-nontarget tissue ratios compared with the same compound at lower SA.

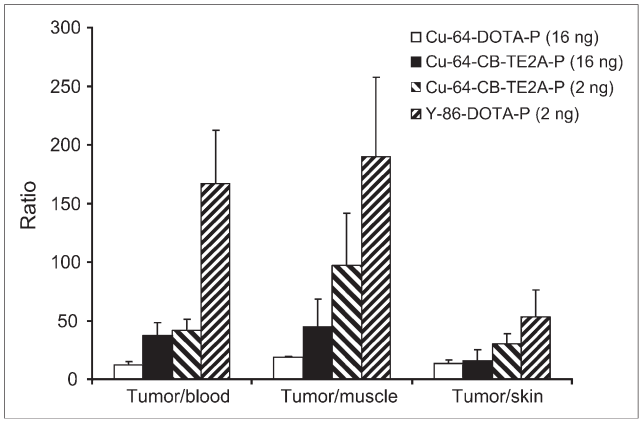

FIGURE 4. Selected tumor-to-organ ratios for ^{64}Cu-DOTA-ReCMSH(Arg^{11}) (*8*), ^{64}Cu-CBTE2A-ReCCMSH(Arg^{11}) with lower and higher SA, and ^{86}Y-DOTA-ReCCMSH(Arg^{11}) (*8*) at 2 h in C57 mice implanted with B16/F1 tumors. (P = ReCCMSH(Arg^{11}).)

Although the tumor-to-nontarget organ ratios of ^{64}Cu-CBTE2A-ReCCMSH(Arg^{11}) (16 ng) are lower compared with ^{86}Y-DOTA-ReCCMSH(Arg^{11}) (1.7 ng) (*8*), expected by the lower SA of the Cu-peptide in this comparison, its tumor retention and kidney clearance are superior to those of ^{86}Y-DOTA-ReCCMSH(Arg^{11}). At 24 h after injection, the tumor concentration of ^{86}Y-DOTA-ReCCMSH(Arg^{11}) is only 6.5% of the 30-min concentration ($P < 0.0001$). For ^{64}Cu-CBTE2A-ReCCMSH(Arg^{11}), the tumor uptake at 24 h after injection is 48% of the 30-min uptake ($P < 0.001$). Kidney uptake is higher for ^{86}Y-DOTA-ReCCMSH(Arg^{11}) than that for ^{64}Cu-CBTE2A-ReCCMSH(Arg^{11}) at all time points. ^{64}Cu-CBTE2A-ReCCMSH(Arg^{11}) demonstrates more rapid kidney clearance compared with ^{86}Y-DOTA-ReCCMSH(Arg^{11}). By 24 h, the ^{64}Cu activity in kidney had fallen to 28% of the 30-min activity for ^{64}Cu-CBTE2A-ReCCMSH(Arg^{11}) ($P < 0.001$), whereas ^{86}Y activity had fallen to 55% of the 30-min activity for ^{86}Y-DOTA peptide analog ($P < 0.005$), resulting in 3.2-fold higher kidney uptake at 24 h for ^{86}Y-DOTA-ReCCMSH(Arg^{11}) ($P < 0.01$).

microPET Images

Small-animal PET images of ^{64}Cu-CBTE2A-ReCCMSH(Arg^{11}) were obtained with C57 mice bearing day-10 B16/F1 murine melanoma tumors. Figure 5A shows the coronal images of the mice at 30 min and at 2, 4, and 24 h after injection of 5.55 MBq (150 μCi) (500 ng) of ^{64}Cu-CBTE2A-ReCCMSH(Arg^{11}). Figure 5B shows the microPET and CT coregistered images (coronal, sagittal, and transaxial views) at 2 h after injection. The images demonstrated that the tumors can be easily visualized after only 30 min and can still be delineated at 24 h after injection. PET images also showed that administering a blockade dose (20 μg CBTE2A-ReCCMSH(Arg^{11})) saturated the α-melanocyte-stimulating hormone (α-MSH) receptors, resulting in dramatic reduction of tumor concentration by such an extent that very little activity can be seen in the tumor at all time points. This indicates the receptor-mediated aspect of the tumor accumulation. It is also evident from the images that low background accumulation is observed except that the kidney uptake is high. SUVs of tumor, kidney, and liver were calculated for both blocked and nonblocked animals (Fig. 6). SUVs indicated that the tumor uptake of the blocked mice is significantly lower than that of nonblocked mice at all time points examined. Statistically, there are no differences in the kidney and liver uptakes between the blocked and nonblocked animals.

DISCUSSION

α-MSH peptide analogs have been suggested as agents for targeting the MC1R expressed on metastatic melanoma. MC1R belongs to a family of G-protein−coupled receptors, of which 5 (MC1R to MC5R) have been isolated in both mice and humans (*19–24*). These receptors are normally expressed on the surface of melanocytes, and

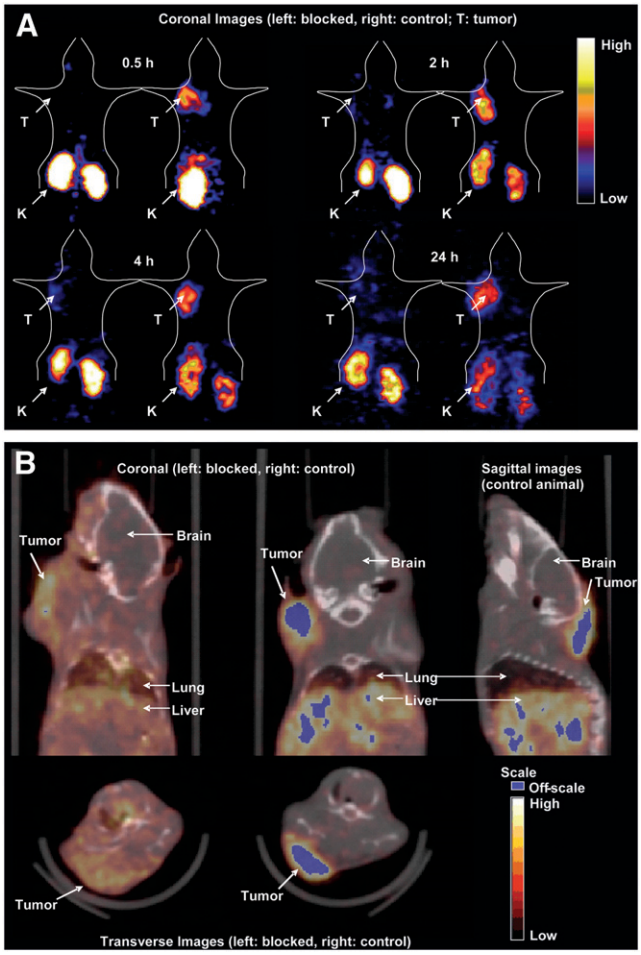

FIGURE 5. (A) Coronal images of C57 mice implanted with B16/F1 tumors at 30 min and at 2, 4, and 24 h after tail vein injection of 5.55 MBq (150 μCi) (500 ng) of ^{64}Cu-CBTE2A-ReCCMSH(Arg^{11}). At each time point a mouse that received blockade (left) was coimaged with a mouse that did not receive blockade (right). Blockade mouse received 20 μg of CBTE2A-ReCCMSH(Arg^{11}). Images shown are 1-mm slices, with animal in supine position, and slices shown are through center of tumor volume. As tumors do not grow in exactly the same location from animal to animal, slices may show different tissues in addition to tumors. PET images show that administration of a blockade dose substantially reduces tumor uptake of the agent by such an extent that tumor is difficult to delineate. It is also evident that background accumulation is very low, resulting in excellent tumor contrast. T = tumor; K = kidney. (B) microPET/CT coregistered images of B16/F1 tumor-bearing mice 2 h after tail vein injection of 5.5 MBq (500 ng) of ^{64}Cu-CBTE2A-ReCCMSH(Arg^{11}). Images shown are 1-mm slices and slices shown are through center of tumor volume.

MC1 was found to be overexpressed on 80% of melanoma cells and tissues (*25*). α-MSH is a tridecapeptide that is primarily responsible for the regulation of skin pigmentation by controlling melanin synthesis and dispersal of melanocytes (*26*). It has been found to bind avidly to MC1R, enabling the use of radiolabeled α-MSH peptide analogs as melanoma-specific diagnostic and therapeutic agents.

Linear α-MSH peptide analogs (DPMSH and NDPMSH) were investigated as potential agents for specific melanoma targeting. When labeled with either ^{99m}Tc or ^{188}Re, these linear peptides showed high uptake and prolonged retention in murine melanoma-bearing mouse models (*27*). A new family of α-MSH analogs was then developed that incorporated the rhenium and technetium directly into the peptide's structure to generate the cyclic α-MSH analog ^{99m}TcO or ReO [Cys^{3,4,10},D-Phe^{7}]-α-MSH$_{3–13}$ [ReCCMSH] (*28–30*). Substitution of Arg^{11} for Lys^{11} in ReCCMSH peptide resulted in the analog ReCCMSH(Arg^{11}), which showed greater tumor uptake and lower kidney accumulation compared with the ReCCMSH (*16,17*). Studies also included conjugation of DOTA to the terminal amine for labeling with 2$^+$- and 3$^+$-charged radiometals for both imaging and therapy purposes (*31*). A series of linear peptide systems has also been examined with ^{111}In and ^{67}Ga via DOTA chelation and has shown good tumor accumulation in animal models of melanoma (*32–36*).

In our previous study, we radiolabeled DOTA-ReCCMSH(Arg^{11}), one of the DOTA-ReCCMSH analogs, with β$^+$-emitting radionuclides ^{64}Cu and ^{86}Y to investigate their potential as PET agents (*8*). Small-animal PET and biodistribution studies indicated that both ^{64}Cu- and ^{86}Y-labeled DOTA-ReCCMSH(Arg^{11}) are promising candidates for the detection of melanoma by taking advantage of the sensitivity and high resolution of PET. However, ^{64}Cu-DOTA-ReCCMSH(Arg^{11}) demonstrated high radioactive accumulation in liver and other nontarget organs. Although DOTA is an excellent chelator for many 2$^+$- and 3$^+$-charged metals, ^{64}Cu has been shown to dissociate in vivo from DOTA and DOTA-conjugates and undergo metabolism and transchelation to superoxide dismutase and other proteins (*12,15*). The cross-bridged cyclam chelator CBTE2A has demonstrated improved in vivo stability and, consequently, a reduction in transchelation (*12,13*). The goal of this project was to synthesize ^{64}Cu-labeled CBTE2A-conjugated ReCCMSH(Arg^{11}) peptide and compare its biologic properties with the ^{64}Cu- and ^{86}Y-DOTA-ReCCMSH(Arg^{11}) analogs.

Acute biodistribution and small-animal PET studies of ^{64}Cu-CBTE2A-ReCCMSH(Arg^{11}) showed high tumor uptake and retention that was similar to the reported tumor uptakes of ^{64}Cu- and ^{86}Y-DOTA-ReCCMSH(Arg^{11}) (*8*). The tumor uptake was dramatically reduced by the coinjection of a blocking dose of CBTE2A-ReCCMSH(Arg^{11}), saturating the α-MSH receptor-binding sites. This strongly confirms a receptor-mediated uptake process for ^{64}Cu-CBTE2A-ReCCMSH(Arg^{11}). The comparison with ^{64}Cu-DOTA-ReCCMSH(Arg^{11}) clearly indicates the superiority of ^{64}Cu-CBTE2A-ReCCMSH(Arg^{11}), and this comparison is valid because the current study was designed so that the identical mass of peptide (16 ng) was administered. Although the tumor concentrations of the 2 compounds are comparable, dramatic differences in the uptake and retention in nontarget tissues were found. There was much lower

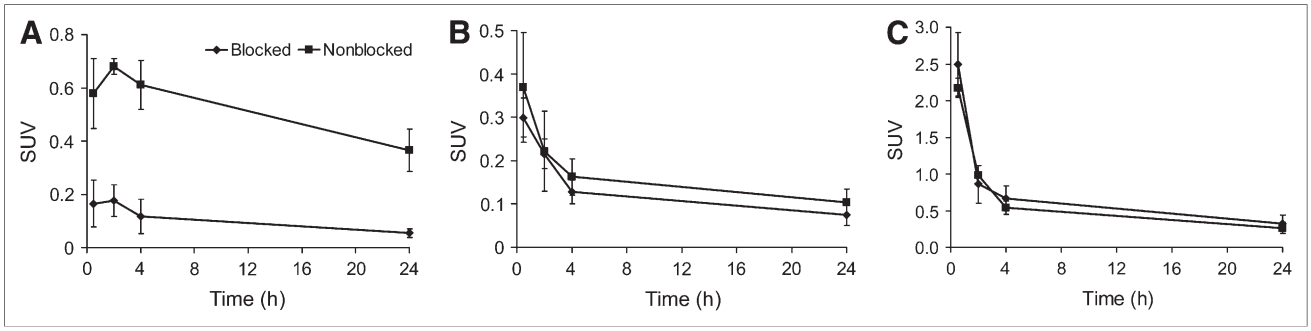

FIGURE 6. SUV data obtained for PET analysis of ^{64}Cu-CBTE2A-ReCCMSH(Arg^{11}) (500 ng) in C57 mice implanted with B16/F1 tumors. Shown are SUVs of uptakes in tumor (A), liver (B), and kidney (C). SUVs for tumor (A) are low due to mass of peptide administered compared with that in biodistribution study (16 ng).

accumulation of ^{64}Cu-CBTE2A-ReCCMSH(Arg^{11}) in nontarget tissues compared with ^{64}Cu-DOTA-ReCCMSH(Arg^{11}) at later time points, indicating improved clearance. The low uptake of ^{64}Cu-CBTE2A-ReCCMSH(Arg^{11}) in nontarget tissues results in superior tumor-to-nontarget organ ratios (Fig. 4) and, consequently, low absorbed radiation doses in nontarget tissues. This reduction in background accumulation is further proved by the high quality of the PET images of ^{64}Cu-CBTE2A-ReCCMSH(Arg^{11}) (Figs. 5A and 5B), where tumor is clearly delineated even after 30 min against low background activity. Similar differences in nontarget tissue biodistribution were found between ^{64}Cu-CBTE2A-Y3-TETA and ^{64}Cu-TETA-Y3-TATE (*12,15*). The lower background of ^{64}Cu-CBTE2A peptides compared with ^{64}Cu-DOTA or ^{64}Cu-TETA analogs confirms that the Cu-CBTE2A chelate is more stable than both the Cu-DOTA and the Cu-TETA chelates and is less susceptible to transchelation in vivo.

It has been reported that the renal retention of ^{64}Cu- and ^{111}In-labeled compounds was higher for positively charged peptides and lower for neutral and negatively charged ones (*37–39*). A recent study also discussed the structural parameters that affect the tumor and kidney uptake of DOTA-MSH analogs (*36*). It was found that the kidney uptake of DOTA-MSH analogs could be considerably reduced, without affecting the affinity for the receptor, by neutralizing the charge of the Lys^{11} residue. The resulting peptides exhibited a high ratio of tumor to kidney uptake that was favorable for both diagnostic and therapeutic applications. According to the structure of the ^{64}Cu-labeled conjugated peptide, the predicted net charges of ^{64}Cu-CBTE2A-ReCCMSH(Arg^{11}) and ^{64}Cu-DOTA-ReCCMSH(Arg^{11}) are +1 and −1, respectively, suggesting that ^{64}Cu-CBTE2A-ReCCMSH(Arg^{11}) should show higher kidney retention. However, to our surprise, ^{64}Cu-CBTE2A-ReCCMSH(Arg^{11}) showed faster kidney clearance compared with ^{64}Cu-DOTA-ReCCMSH(Arg^{11}). Therefore, we hypothesize that the peptide backbone of ^{64}Cu-CBTE2A-ReCCMSH(Arg^{11}) may be deprotonated in vivo to change the net charge of the entire complex to neutral or even negative, resulting in lower renal retention.

The biodistribution of ^{64}Cu-CBTE2A-ReCCMSH(Arg^{11}) was clearly affected by the mass of the injected peptide. Increasing SAs from 22.2 to 185 GBq/μmol reduced the mass of the peptide injected in the acute biodistribution studies from 16 to 2 ng, resulting in a significant increase in tumor concentration and more favorable tumor-to-nontarget tissue ratios. An expected reduction in tumor uptake was noted in the imaging studies where administration of 500 ng of peptide, although still allowing for excellent tumor delineation, resulted in a low SUV (SUV, 0.68 ± 0.03; ~3 %ID/g). This is still a 3-fold higher value than that obtained when a blocking dose (20 μg CBTE2A-ReCCMSH(Arg^{11})) was administered. The tumor uptake at 2 h after injection of ^{64}Cu-CBTE2A-ReCCMSH(Arg^{11}) (2 ng) was 22.59 ± 2.99 %ID/g, which is the highest tumor concentration compared with previously reported ^{64}Cu-, ^{86}Y-, and ^{111}In-labeled DOTA-ReCCMSH(Arg^{11}) (*8,31*).

The nonspecific radioactivity accumulation in the kidneys often hinders the in vivo application of radiolabeled peptides and antibody fragments. Studies have shown that lysine administration can result in a significant reduction of ^{111}In-DTPA-octreotide (DTPA is diethylenetriaminepentaacetic acid) in the kidneys without affecting uptake in receptor-positive tissues (*40*). Lysine coinjection was shown to decrease the kidney uptake without significantly interfering with the high melanoma-targeting properties of ^{99m}Tc-CCMSH (*29*). Our results indicated that administration of D-lysine dramatically reduced the kidney uptake while the radioactivity accumulation in other organs demonstrated no significant change. However, the tumor concentration was also decreased by the same extent as the reduction of the kidney uptake. This may be related to the lysine administration methods and doses. In the current study, lysine was injected before the injection of ^{64}Cu-CBTE2A-ReCCMSH(Arg^{11}), whereas in the reported studies, lysine was coinjected with the radiopharmaceuticals.

CONCLUSION

^{64}Cu-CBTE2A-ReCCMSH(Arg^{11}) was evaluated as an agent for the PET of malignant melanoma. These data

suggest the superior Cu-chelating property of CBTE2A compared with DOTA, resulting in much improved liver and blood clearance as well as higher tumor-to-nontarget tissue ratios for ^{64}Cu-CBTE2A-ReCCMSH(Arg^{11}). A comparison with ^{86}Y-DOTA-ReCCMSH(Arg^{11}) clearly indicated the prolonged tumor retention and more rapid renal clearance of ^{64}Cu-CBTE2A-ReCCMSH(Arg^{11}). Therefore, ^{64}Cu-CBTE2A-ReCCMSH(Arg^{11}) is a promising melanoma-targeting agent for clinical application as a diagnostic PET agent for malignant melanoma.

ACKNOWLEDGMENTS

We thank Dr. Gary R. Weisman and Dr. Edward H. Wong for supplying the CBTE2A. We are very grateful for the technical assistance of Lori Strong, Nicole Fettig, Dawn Werner, Margaret Morris, and Jerrel Rutlin. This work was partially supported by the National Cancer Institute (NCI) (grants R24 CA86307 and P50 CA103130). Small-animal PET is supported by an NIH/NCI SAIRP grant (R24 CA86060) with additional support from the Small Animal Imaging Core (SAIC) of the Alvin J. Siteman Cancer Center at Washington University and Barnes-Jewish Hospital. The SAIC is supported by an NCI Cancer Center Support grant (P30 CA91842).

REFERENCES

1. Vosmik F. Malignant melanoma of the skin: epidemiology, risk factors, clinical diagnosis. *Cas Lek Cesk.* 1996;135:405–408.
2. Dennis LK. Analysis of the melanoma epidemic, both apparent and real: data from the 1973 through 1994 surveillance, epidemiology, and end results program registry. *Arch Dermatol.* 1999;135:275–280.
3. Dennis LK. Increasing risk of melanoma with increasing age. *JAMA.* 1999; 282:1037–1038.
4. Jemal A, Tiwari RC, Murray T, et al. Cancer Statistics 2004. *CA Cancer J Clin.* 2004;54:8–29.
5. Som P, Atkins HL, Bandoypadhyay D, et al. A fluorinated glucose analog, 2-fluoro-2-deoxy-D-glucose (F-18): nontoxic tracer for rapid tumor detection. *J Nucl Med.* 1980;21:670–675.
6. Mijnhout GS, Hoekstra OS, van Tulder MW, Teule GJ, Deville WL. Systematic review of the diagnostic accuracy of ^{18}F-fluorodeoxyglucose positron emission tomography in melanoma patients. *Cancer.* 2001;91:1530–1542.
7. Dimitrakopoulou-Strauss A, Strauss LG, Burger C. Quantitative PET studies in pretreated melanoma patients: a comparison of 6-[^{18}F]fluoro-L-DOPA with ^{18}F-FDG and ^{15}O-water using compartment and noncompartment analysis. *J Nucl Med.* 2001;42:248–256.
8. McQuade P, Miao Y, Yoo J, Quinn TP, Welch MJ, Lewis JS. Imaging of melanoma using ^{64}Cu- and ^{86}Y-DOTA-ReCCMSH(Arg^{11}), a cyclized peptide analogue of α-MSH. *J Med Chem.* 2005;48:2985–2992.
9. Blower PJ, Lewis JS, Zweit J. Copper radionuclides and radiopharmaceuticals in nuclear medicine. *Nucl Med Biol.* 1996;23:957–980.
10. McCarthy DW, Shefer RE, Klinkowstein RE, et al. Efficient production of high specific activity ^{64}Cu using a biomedical cyclotron. *Nucl Med Biol.* 1997;24:35–43.
11. Yoo J, Tang L, Perkins TA, et al. Preparation of high specific activity ^{86}Y using a small biomedical cyclotron. *Nucl Med Biol.* 2005;32:891–897.
12. Boswell CA, Sun X, Niu W, et al. Comparative in vivo stability of copper-64-labeled cross-bridged and conventional tetraazamacrocyclic complexes. *J Med Chem.* 2004;47:1465–1474.
13. Sun X, Wuest M, Weisman GR, et al. Radiolabeling and in vivo behavior of copper-64-labeled cross-bridged cyclam ligands. *J Med Chem.* 2002;45: 469–477.
14. Wong EH, Weisman GR, Hill DC, et al. Synthesis and characterization of cross-bridged cyclams and pendant-armed derivatives, and structural studies of their copper(II) complexes. *J Am Chem Soc.* 2000;122:10561–10572.
15. Sprague JE, Peng Y, Sun X, et al. Preparation and biological evaluation of copper-64-labeled Tyr^3-octreotate using a cross-bridged macrocyclic chelator. *Clin Cancer Res.* 2004;10:8674–8682.
16. Miao Y, Owen NK, Whitener D, Gallazzi F, Hoffman TJ, Quinn TP. In vivo evaluation of ^{188}Re-labeled α-melanocyte stimulating hormone peptide analogs for melanoma therapy. *Int J Cancer.* 2002;101:480–487.
17. Cheng Z, Chen J, Quinn TP, Jurisson SS. Radioiodination of rhenium cyclized α-melanocyte-stimulating hormone resulting in enhanced radioactivity localization and retention in melanoma. *Cancer Res.* 2004;64:1411–1418.
18. Tai YC, Ruangma A, Rowland DJ, et al. Performance evaluation of the microPET Focus: a third-generation microPET scanner dedicated to animal imaging. *J Nucl Med.* 2005;46:455–463.
19. Eves PC, MacNeil S, Haycock JW. α-Melanocyte stimulating hormone, inflammation and human melanoma. *Peptides.* 2006;27:444–452.
20. Gantz I, Konda Y, Tashiro T, et al. Molecular cloning of a novel melanocortin receptor. *J Biol Chem.* 1993;268:8246–8250.
21. Gantz I, Miwa H, Konda Y, et al. Molecular cloning, expression, and gene localization of a fourth melanocortin receptor. *J Biol Chem.* 1993;268:15174–15179.
22. Barrett P, MacDonald A, Helliwell R, Davidson G, Morgan P. Cloning and expression of a new member of the melanocyte-stimulating hormone receptor family. *J Mol Endocrinol.* 1994;12:203–213.
23. Desarnaud F, Labbe O, Eggerickx D, Vassart G, Parmentier M. Molecular cloning, functional expression and pharmacological characterization of a mouse melanocortin receptor gene. *Biochem J.* 1994;299:367–373.
24. Labbe O, Desarnaud F, Eggerickx D, Vassart G, Parmentier M. Molecular cloning of a mouse melanocortin 5 receptor gene widely expressed in peripheral tissues. *Biochemistry.* 1994;33:4543–4549.
25. Tatro JB, Wen Z, Entwistle ML, et al. Interaction of an α-melanocyte-stimulating hormone-diphtheria toxin fusion protein with melanotropin receptors in human melanoma metastases. *Cancer Res.* 1992;52:2545–2548.
26. Hruby VJ, Sharma SD, Toth K, et al. Design, synthesis, and conformation of superpotent and prolonged acting melanotropins. *Ann N Y Acad Sci.* 1993;680: 51–63.
27. Chen J, Giblin MF, Wang N, Jurisson SS, Quinn TP. In vivo evaluation of ^{99m}Tc/^{188}Re-labeled linear α-melanocyte stimulating hormone analogs for specific melanoma targeting. *Nucl Med Biol.* 1999;26:687–693.
28. Giblin MF, Wang N, Hoffman TJ, Jurisson SS, Quinn TP. Design and characterization of α-melanotropin peptide analogs cyclized through rhenium and technetium metal coordination. *Proc Natl Acad Sci U S A.* 1998;95:12814-12818.
29. Chen J, Cheng Z, Hoffman TJ, Jurisson SS, Quinn TP. Melanoma-targeting properties of ^{99m}technetium-labeled cyclic α-melanocyte-stimulating hormone peptide analogues. *Cancer Res.* 2000;60:5649–5658.
30. Chen J, Cheng Z, Owen NK, et al. Evaluation of an ^{111}In-DOTA-rhenium cyclized α-MSH analog: a novel cyclic-peptide analog with improved tumor-targeting properties. *J Nucl Med.* 2001;42:1847–1855.
31. Cheng Z, Chen J, Miao Y, Owen NK, Quinn TP, Jurisson SS. Modification of the structure of a metallopeptide: synthesis and biological evaluation of ^{111}In-labeled DOTA-conjugated rhenium-cyclized α-MSH analogues. *J Med Chem.* 2002; 45:3048–3056.
32. Eberle AN, Froidevaux S. Radiolabeled α-melanocyte-stimulating hormone analogs for receptor-mediated targeting of melanoma: from tritium to indium. *J Mol Recognit.* 2003;16:248–254.
33. Froidevaux S, Calame-Christe M, Tanner H, Sumanovski L, Eberle AN. A novel DOTA-α-melanocyte-stimulating hormone analog for metastatic melanoma diagnosis. *J Nucl Med.* 2002;43:1699–1706.
34. Froidevaux S, Calame-Christe M, Sumanovski L, Tanner H, Eberle AN. DOTA α-melanocyte-stimulating hormone analogues for imaging metastatic melanoma lesions. *Ann N Y Acad Sci.* 2003;994:378–383.
35. Froidevaux S, Calame-Christe M, Schuhmacher J, et al. A gallium-labeled DOTA-α-melanocyte-stimulating hormone analog for PET imaging of melanoma metastases. *J Nucl Med.* 2004;45:116–123.
36. Froidevaux S, Calame-Christe M, Tanner H, Eberle AN. Melanoma targeting with DOTA-α-melanocyte-stimulating hormone analogs: structural parameters affecting tumor uptake and kidney uptake. *J Nucl Med.* 2005;46:887–895.
37. Akizawa H, Arano Y, Mifune M, et al. Effect of molecular charges on renal uptake of ^{111}In-DTPA-conjugated peptides. *Nucl Med Biol.* 2001;28:761–768.
38. Rogers BE, Anderson CJ, Connett JM, et al. Comparison of four bifunctional chelates for radiolabeling monoclonal antibodies with copper radioisotopes: biodistribution and metabolism. *Bioconjug Chem.* 1996;7:511–522.
39. Jones-Wilson TM, Deal KA, Anderson CJ, et al. The in vivo behavior of copper-64-labeled azamacrocyclic complexes. *Nucl Med Biol.* 1998;25:523–530.
40. Bernard BF, Krenning EP, Breeman WAP, et al. D-Lysine reduction of indium-111 octreotide and yttrium-90 octreotide renal uptake. *J Nucl Med.* 1997;38: 1929–1933.